Digital Manufacturing Technology
https://ojs.wiserpub.com/index.php/DMT/

UNIVERSAL WISER PUBLISHER

Research Article

Paper presented in the special issue of [Advanced Materials in Additive Manufacturing]

Investigation of the Process-Induced Defects in Metal Fused Deposition Modeling Process of Ultrafuse 316L Stainless Steel

Abbas Raza[1], Syed Waqar Ahmed[1*], Adeel Hassan[1], Khurram Altaf[1], Hongyu Wei[2], Ghulam Hussain[3]

[1]Department of Mechanical Engineering, Universiti Teknologi PETRONAS, Perak Darul Ridzuan 32610, Malaysia
[2]College of Mechanical & Electrical Engineering, Nanjing University of Aeronautics & Astronautics, Nanjing 210016, PR China
[3]Mechanical Engineering Department, College of Engineering, University of Bahrain, Isa town 32038, Kingdom of Bahrain
E-mail: syed_19000908@utp.edu.my

Received: 27 July 2023; **Revised:** 2 October 2023; **Accepted:** 5 October 2023

Abstract: The current article presents a case study of the defects that can occur in the metal fused deposition modeling (FDM) process, a popular additive manufacturing technique for producing metal parts. The metal parts of Ultrafuse 316L SS filament (a metal-polymer composite) were produced and then subjected to de-binding and sintering. The defects in the brown parts (after de-binding) and the silver parts (after sintering) were analyzed carefully. The main defects detected include brittleness, cracks, blisters, layer delamination, part deformation, and porosity. Further, the formation of these defects was found to be influenced by the process parameters such as heating rate, holding time, temperature, and atmosphere. The analysis of these effects suggests to use furnace temperature of 310 °C, heating rate of 1 °C/min and holding time of around 10 to 15 minutes to minimize the defects. As regard to the atmosphere, vacuum is preferred over other environments to produce parts with reduced defects and enhanced quality.

***Keywords*:** fused deposition modeling, 3D printing, additive manufacturing, metal printing, de-binding, sintering, Ultrafuse 316L SS

1. Introduction

The fabrication of metal parts encompasses a range of manufacturing processes, which can be broadly classified into three categories: subtractive manufacturing (SM), forming manufacturing (FM), and additive manufacturing (AM). SM involves the removal of material through machining techniques such as grinding, milling, and cutting [1]. In contrast, FM entails the pouring of molten material into molds, allowing it to solidify and acquire the desired shape upon cooling [2]. AM, as defined by ISO/ASTM 52900:2017, involves the layer-by-layer joining of materials based on instructions from a 3D model [3].

In recent years, AM has experienced remarkable growth in various industries worldwide, including automotive, biomedical, aerospace, and agriculture, while still being in its nascent stage [4]. The distinguishing feature of AM lies in its ability to fabricate highly complex geometries, surpassing the limitations of traditional manufacturing methods [5]. Additionally, its customization and personalization capabilities have positioned it as a crucial pillar of Industry 4.0 [6]. By combining different raw materials and intricate designs in an economical manner, AM enables the production

DOI: https://doi.org/10.37256/dmt.3220233447

of homogenous and heterogeneous products with unprecedented flexibility. Among the diverse range of AM processes, fused deposition modeling (FDM) has emerged as a popular choice, especially due to its cost-effectiveness, design freedom, waste reduction, and economic viability [7]. While initially associated with plastic products, FDM has extended its applicability to the fabrication of ceramics and even metal parts [8-10].

Moreover, it is crucial to acknowledge that the metal FDM process comes with certain limitations and disadvantages. Despite being a cost-effective technique compared to other AM methods such as selective laser melting (SLM), electron beam melting (EBM), and binder jetting (BJ), metal parts produced through FDM exhibit relatively low mechanical strength owing to process induced defects in the parts. This limitation can be attributed to the inherent anisotropy found in FDM-manufactured metal parts, resulting in variations in mechanical properties depending on the orientation of the printing layers [6].

Various researchers have utilized FDM for the production of metal parts and investigated both the manufacturing process and the integrity of the final products. A study conducted by Wu et al. [11] explored the fused deposition of metals (FDMet) technique as a hard tooling fabrication method for prototype metal components, eliminating the need for molds or dies. The process, based on FDM principles and employing a metal filament, enables direct three-dimensional object fabrication. Post-processing steps involving binder removal and sintering result in densification. The technique demonstrated success in producing standard samples and hard tooling components. However, for broader applicability, improvements in accuracy, reproducibility, and defect elimination could be essential areas of focus. It was concluded that FDMet holds promise as an efficient and cost-effective approach for rapid metal component prototyping. Kurose et al. [12] used the FDMet technique with a 316L stainless steel particle-filled filament and organic binder to produce metal specimens. Investigations on processing conditions revealed that a layer thickness of 0.1 mm resulted in higher relative densities (92.9%) compared to 0.3 mm. Anisotropic shrinkage was observed, with the highest linear shrinkage along the layer direction (15-17%). Mechanical properties varied depending on the layer direction, with the perpendicular direction showing the highest ultimate strength (453 MPa) and strain at break (48%). Researchers observed that anisotropy was attributed to segregated binder domains and oriented binder domains in the green parts, influencing metal particle distance during sintering. It was concluded that addressing the defects such as anisotropy, is vital for commercialization of the FDMet process for small-sized metal parts [12].

Zhang and Roch [13] demonstrates the competitiveness of fused filament fabrication (FFF) in AM of 17-4PH metal parts. Highly dense material with relatively improved mechanical properties were noted, including a yield strength of 1007 MPa and ultimate strength of 1212 MPa, similar to conventional MIM 17-4PH materials. Therefore, FFF offers economic advantages, simplicity, and minimal safety standards. Proper printer settings and sintering are crucial for part performance. The growing availability of FFF filaments makes it a highly competitive and promising technology for future applications. Safka et al. [14] aimed to directly compare the FFF manufactured Ultrafuse 316LX material with rolled material and SLM processed specimens. The feasibility of using FFF for producing fully functional metallic parts was also evaluated. The study found that inexpensive desktop printers can be used for fabricating metallic models, making initial investment affordable for many companies. However, specific equipment for de-binding and sintering is required for post-processing, which can increase the overall cost. Tensile tests showed that the Ultrafuse 316LX material had lower ultimate tensile stress and yield stress compared to rolled 316L material but offered greater ductility. These materials show promising possibilities for further research and development, including investigating properties such as shrinkage, shape precision, porosity, and conducting deeper material-related analyses. Obadimu and Kourousis [15] evaluated the influence of fabrication parameters on the microscopic and mesoscopic/macroscopic characteristics of material extrusion (ME) Steel 316L parts and their impact on structural integrity. The study highlighted the heterogeneity of grain structures and the presence of voids and porosities in ME metal parts, resulting from production-induced defects such as incomplete fusion and inadequate extrusion. It was observed that the de-binding and sintering processes also affect the microstructural and mesostructural/macrostructural characteristics, further compromising structural integrity and leading to mechanical anisotropy. Controlling the ME fabrication process, including manufacturing parameters and de-binding/sintering conditions, is crucial to minimize variations in microstructure and porosity, thus enhancing structural integrity. Researchers recommended further research to optimize fabrication parameters and improve the understanding of their impact on ME Steel 316L parts.

In view of the literature presented above, it can be concluded that metal parts fabricated using the FDM process often exhibit higher levels of porosity and inherit process induce defects when compared to similar parts produced

through alternative metal AM processes. The increased porosity and inherent defects negatively impact crucial mechanical properties, including tensile strength, bending strength, and yield strength. The extent of defects in FDM-produced metal parts is highly influenced by parameters related to printing, de-binding, and sintering. The post-processing parameters play a vital role in eliminating the induced defects which directly influence the overall mechanical performance of the metal parts. As the technology surrounding metal FDM continues to evolve and advance, it is imperative to address potential defects that may arise during the process. To the best of authors' knowledge, there are very limited studies [16, 17] that discuss the FDM related process induce defects and therefore it is need of the time to present and discuss the defects. Consequently, the focus of this paper is to present a comprehensive case study and thoroughly examine the defects that can occur during the metal FDM process.

2. Materials and methods

In this study, the research material used was a metal-polymer composite filament, Ultrafuse 316L SS, with a diameter of 2.85 mm. The material was chosen for its favorable mechanical and biocompatible properties and was sourced from BASF, USA. An Ultimaker S5 machine was employed to create 3D printed specimens, called as green parts, following the MPIF-35 standard using the FDM method. The printing parameters, including layer height, printing speed, infill type, and infill density, were carefully selected and are listed in Table 1. It is noteworthy that the Ultrafuse 316L SS filament being a composite that contains 80% of stainless-steel particles is highly abrasive in nature, therefore the general-purpose print core (AA 0.4) is not recommended [18]. Instead, the special print core (CC 0.4) which is made of hardened steel was employed for 3D printing as recommended by Ultimaker. It was recommended by the Ultrafuse 316L SS filament manufacturer to scale the part up by 120% in the X and Y, and 126 % scale up in the Z direction for printing. Figure 1 displays the actual manufactured green part along with the printing setup. A total of 18 FDM printed samples were initially fabricated for subsequent post-processing.

Table 1. Green part printing parameters

Printing parameters	Values
Nozzle material	Hardened steel
Nozzle diameter	0.40 mm
Layer height	0.1 mm
Extrusion temperature	230-250 °C
Bed temperature	90-100 °C
Infill density	100%
Infill type	Hatch 45°
Print speed	50-60 mm/s

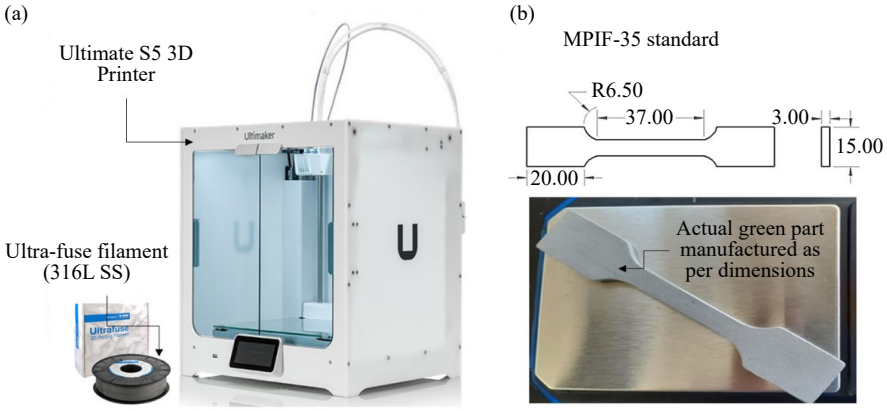

Figure 1. Green part manufacturing illustration: (a) FDM 3D printing setup; (b) green part geometry and actual 3D printed part

The green parts were then followed by de-binding process in which binder removal is carried out and the obtained part is called as brown part. To achieve brown parts, green parts were subjected to a combined thermal de-binding and sintering cycle in the tube furnace. Combined thermal de-binding and sintering cycle is shown in Figure 2 and the process parameters are provided in Table 2 respectively. The sintering cycle in Figure 2 that has been employed for the current study, shares similarities with the sintering process applied to 316L SS metal parts via powder metallurgy, as evident in [19]. Since our study utilizes Ultrafuse 316L SS filament, this sintering cycle is well-suited as a reference.

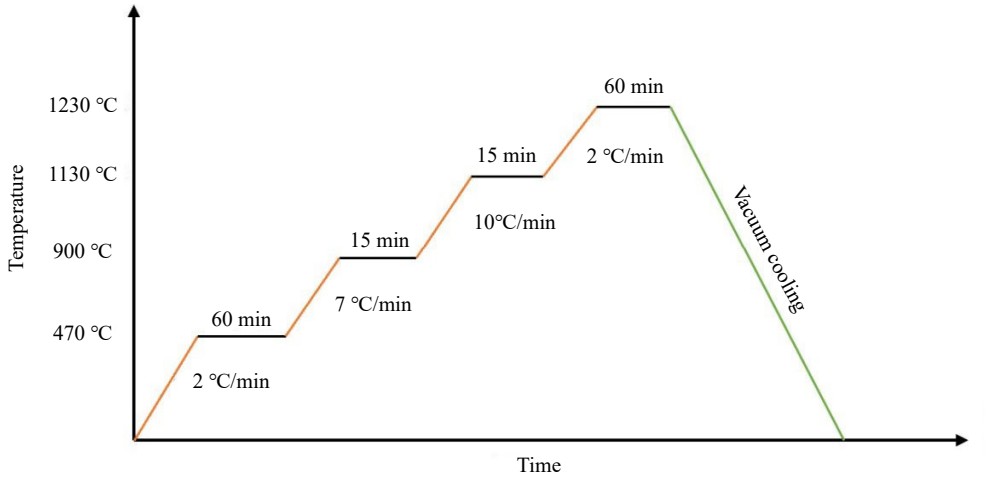

Figure 2. Combined de-binding and sintering cycle [19]

Table 2. Thermal de-binding parameters for different atmospheres

	Nitrogen atmosphere	Vacuum atmosphere	Normal atmosphere (air)
Pressure	1.1 bar	-0.75 bar	-
Input heat rate	20 °C/min	20 °C/min	2 °C/min
De-binding temperature	310 °C	310 °C	340 °C
Holding time	15 min	15 min	10 min
Heat rate after holding	1.5 °C/min, 1 °C/min	1.5 °C/min, 1 °C/min	1 °C/min and 10 min holding time

After analyzing the micro and macro defects produced in the brown parts, the defects free brown parts were further sintered to analyze the defects generated in the final silver parts (fully metallic parts). Sintering was employed under argon and vacuum atmosphere at varying heating rate and holding time. The sintered parts were cooled down under vacuum rather than normal atmosphere. The sintering setup used to conduct experiments is shown in the Figure 3. Figure 4 illustrates the adapted sintering cycle, specifically designed to explore the impact of dwell time on the defects in metal parts produced the sintering process. Overall, a complete transformation of the actual 3D green part to the brown part and then eventually silver part is shown below in Figure 5. At the final stage, the final silver parts were ready for defect analysis which occurred during the process. It is essential to recognize that the processing steps are sequential in nature, meaning that any error, defect, or problem in one step will affect the subsequent steps. Therefore, addressing all issues related to each specific step is crucial for achieving overall success in the process.

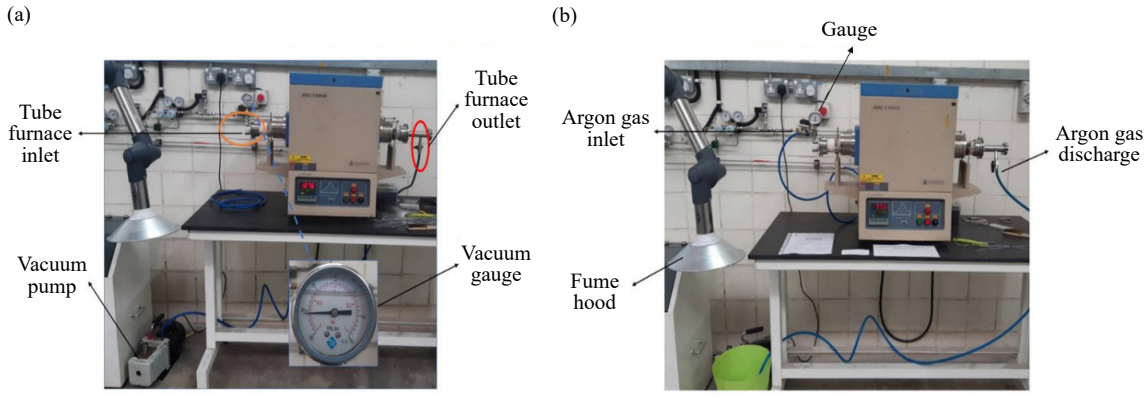

Figure 3. Actual sintering setup: (a) sintering under vacuum atmosphere; (b) sintering under argon atmosphere

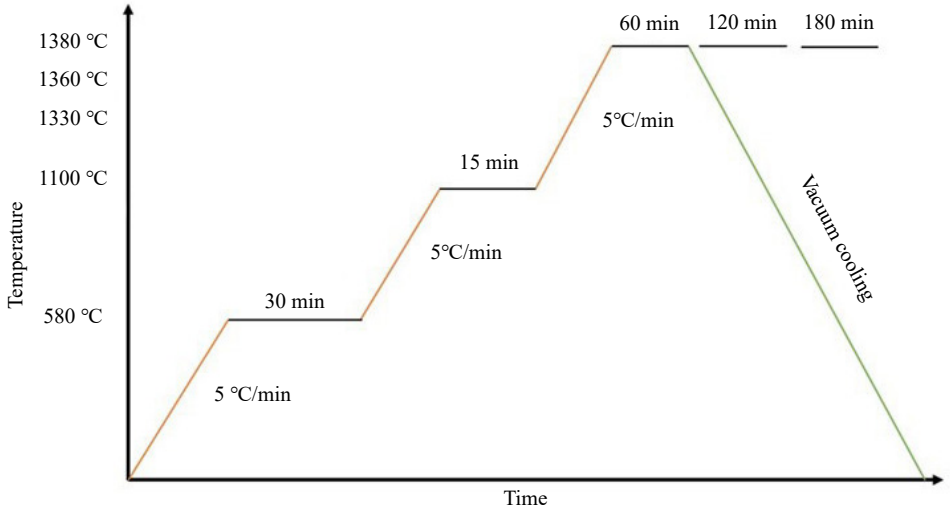

Figure 4. Sintering cycle

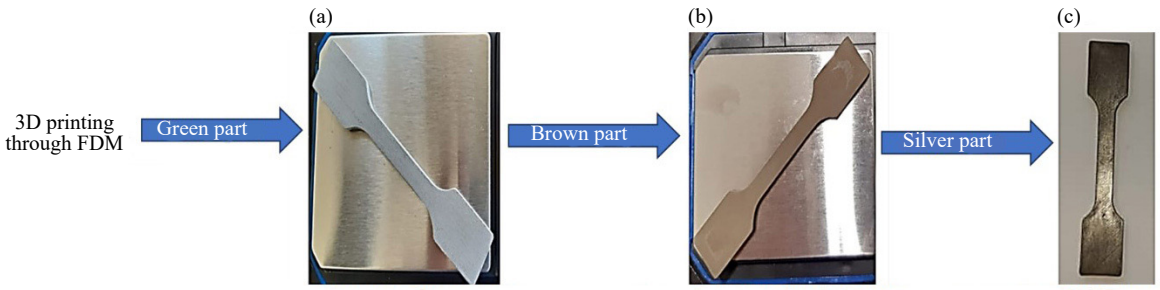

Figure 5. Overview of complete transformation from 3D printing to final metallic part

3. Results and discussion

3.1 *Defects in brown parts*

The brown parts were observed to suffer from two main defects: (a) brittleness; (b) surface cracks during binder removal, as can be seen in Figure 6. The appearance and severity of these defects were found to depend on the processing conditions. The brittleness of the brown parts is regarded as a defect because it makes them very fragile and susceptible to fracture under minor impacts. Actually, the binder is eliminated at this stage (after de-binding) due to which the metal particles are weakly bonded to withstand external forces.

The de-binding was performed in three different environments, namely nitrogen, vacuum and normal. Initially, the de-binding atmosphere was Nitrogen with a heating rate of 2 °C/min until 330 °C and a holding time of 15 minutes. However, cracks appeared on the surface of the brown parts. The probable reason for the cracks on the brown part surface is less dwell time for the removal of binder under high temperature. The de-binding process was repeated by changing environment from nitrogen to vacuum, while the other parameters were kept constant, i.e., heating rate of 2 °C/min and temperature of 330 °C. But the brown part still had blisters and cracks on the surface.

The formation of surface crack on the brown parts appeared as a major challenge thereby calling for further experimentation to enhance and refine the process parameters to mitigate the defects. Therefore, in the next stage, the holding time was extended from 15 to 30 minutes and the furnace temperature was kept same (330 °C) under nitrogen atmosphere. However, these modifications further worsened the situation resulting into significant warpage of the brown parts. A thorough analysis revealed that the brown parts underwent extensive over de-binding and consequently fractured during the process under nitrogen and vacuum atmospheres due to high holding time and temperature. Therefore, it was concluded that these factors (de-binding temperature of 330 °C, holding time more than 10 minutes, and non-feasible thermal de-binding atmosphere) were the main contributors to the defect formation in the brown parts.

Based on these previous findings, that high holding time, high temperature and nitrogen environment cause defects in brown parts, a new set of process parameters was tested under normal atmospheric conditions without nitrogen. The heating rate, holding time and temperature were reduced to 10 °C/min, 10 minutes and 310 °C, respectively. The brown parts obtained from this experiment showed no signs of cracks and had good structural quality. Therefore, these parameters along with normal atmospheric environment were considered appropriate for the debonding process of the green parts.

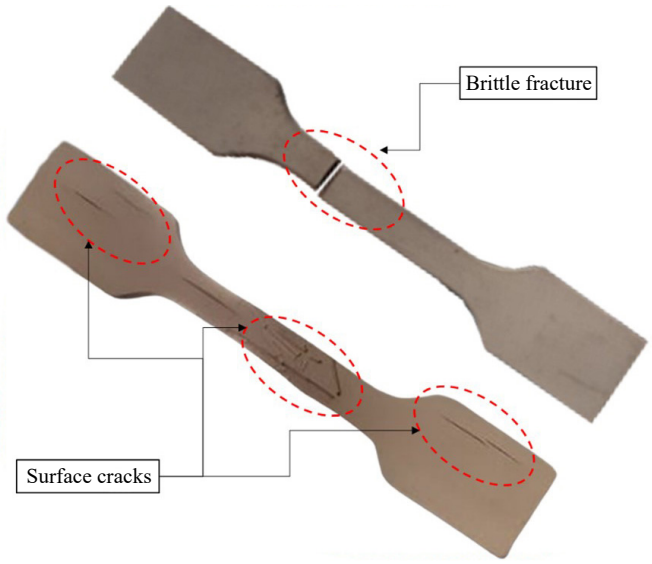

Figure 6. Representation of brittle fracture and surface cracks in brown parts

3.2 *Defects in silver parts*

The green part undergoes de-binding to remove the binder material, followed by sintering to densify the powder and form the silver part. However, some defects may occur during these processes, such as: (a) layer delamination, (b) part deformation, (c) sintering porosity, and (d) cracks or blisters. Figure 7 illustrates an example of layer delamination in the sintered silver part. This defect could be attributed to incomplete de-binding of the brown part, which leaves some residual binder that flows out through the inter-layer boundaries during sintering. Consequently, the layers lose their cohesion and separate from each other, resulting in defective silver parts.

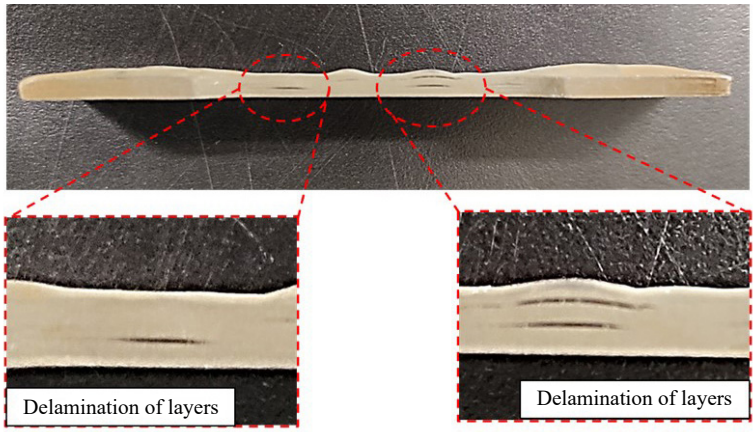

Figure 7. Layer delamination during sintering process

Figure 8 shows the deformation and warpage of the silver parts caused by inappropriate sintering practices. This defect typically arises from non-uniform heating during sintering, which can be induced by the asymmetric placement of insulation blocks inside the tube furnace on either side of the brown part, which is usually located at the furnace centre. This defect may also occur when attempting to sinter a batch of brown parts, which would experience different shrinkage rates due to non-uniform heating, leading to deformation. The red dashed lines indicate the desired shape of the sintered silver parts. However, it can be seen that non-uniform shrinkage has caused distortion of the silver parts, creating undesirable defects.

Figure 8. Deformed specimen due to non-uniform heating

Porosity is one of the most critical defects that can adversely affect the mechanical properties of the sintered silver part. As previously mentioned, the Ultrafuse 316L SS filament contains binder material that holds the metal particles together. The binder material must be eliminated during de-binding, which can be done by thermal, solvent, or catalytic methods. Figure 9 clearly depicts the presence of unburnt residual binder fragments that create significant pores in the sintered silver part. It occurs due to low sintering temperature and insufficient holding time, which prevent adequate fusion between the adjacent metal particles and thus induce porosity. The excessive porosity reduces the shrinkage in the final metal parts, leading to poor inter-particle bonding and lower mechanical strength of the sintered silver part [20].

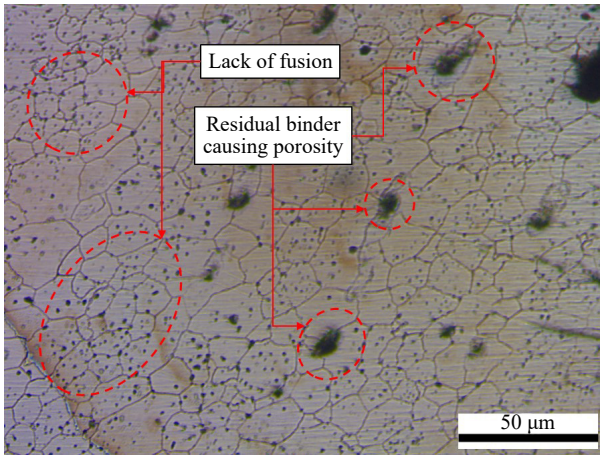

Figure 9. Representation of porosity and lack of fusion at the micro-scale in sintered part

The silver parts exhibit macro-defects, ranging from 250 µm to 400 µm, due to incomplete binder elimination during de-binding phase, as shown in Figure 10. The remaining binder produces gas at high temperatures and creates internal pressure in the material, resulting in surface blisters. This is followed by the layer detachment and formation of macro-cracks if the inter-layer bonding is weak, as evidenced by the micro-graphs in Figure 10. Only gas-enclosed pores are formed when the residual binder content is very small. This occurs due to high heating rate and low holding time, which does not allow the binder to flow out completely. The same phenomenon was observed by Thompson et al. [21] and it is suggested to employ heat rate of 1 °C/min to avoid blisters formation on the bulk material. Macro-cracks were also evident for [17] after the sintering proves that adversely effected the load-bearing area. Likewise, macro-cracks were visible for the current specimen, thus representing the lack of fusion among the adjacent layers.

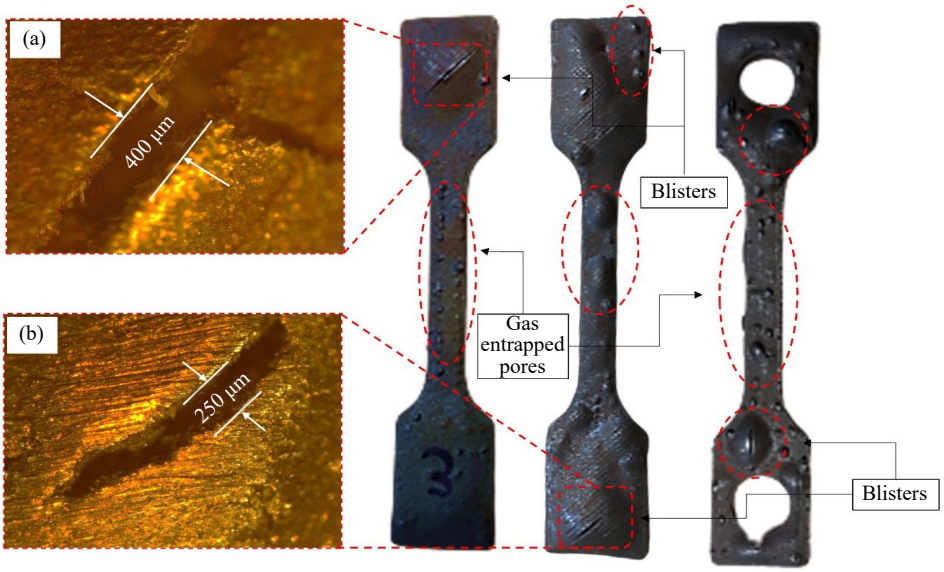

Figure 10. Micrographs of blisters and pores in silver parts

Figure 11 shows a comparison of porosities for specimens sintered in argon, vacuum, and literature. The specimens sintered in argon have high porosity because argon is not soluble in SS 316L matrix and gets trapped between metallic particles, creating voids. The specimens sintered in vacuum have low porosity because there is no gas involved and the likelihood of gas entrapment is very low, leading to higher density and shrinkage. The porosity in the sintered parts is also influenced by the presence of volatile impurities that vaporize during sintering and leave behind micro-pores. The amount of porosity depends on the sintering temperature, time and pressure conditions. Furthermore, porosity can also result from surface oxides or contaminants in the material that hinder bonding and densification during sintering. Therefore, achieving 100% dense part through this process is very difficult. To calculate the porosity in silver parts, the following equation was used:

$$\text{Porosity}\,(\%) = \left(1 - \frac{\rho s}{\rho t}\right) \times 100 \tag{1}$$

where ρs and ρt are density of sintered parts and theoretical density of 316L SS, respectively. The reference density of 316L SS is 7.85 g/cm.

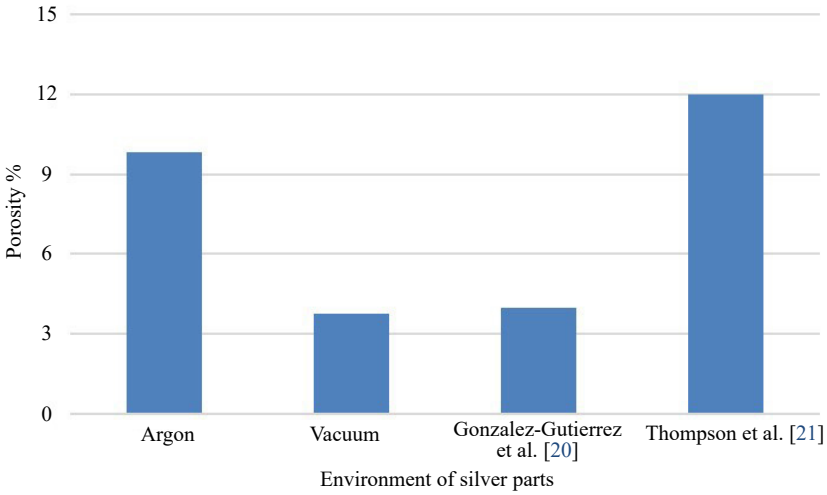

Figure 11. Porosity of silver parts

The above discussion has demonstrated that the improved process parameters for de-binding and sintering of Ultrafuse 316L SS filament are low furnace temperature (310 °C), low heating rate (1 °C/min), and moderate holding time (10 minutes), can reduce the defects in the final silver parts. However, the process still exhibits inherent defects that affect the part quality and performance. Therefore, a potential direction for future research is to separate the de-binding and sintering cycles and apply different parameters for each cycle, which may enhance the defect mitigation and quality improvement in metal FDM process. Furthermore, optimization of the process parameters would yield a more systematic preview on reduction of the defects in the metal FDM technique.

4. Conclusions

The metal FDM process is a promising technique for producing metal parts with complex geometries and high design freedom. However, the process is prone to various defects that can compromise the structural integrity and mechanical properties of the final parts. A detailed case study is presented encompassing the defects that can occur during the metal FDM process using Ultrafuse 316L SS filament as the research material. Defects in the brown part (after de-binding) and silver part (after sintering) are analyzed and the main causes of defects such as incomplete binder removal, non-uniform heating, residual binder fragments, gas entrapment, surface oxides, and impurities, are identified. The study on the effects of process parameters such as heating rate, holding time, temperature, and atmosphere on defect formation has recommended to use furnace temperature of 310 °C, heating rate of 1 °C/min with holding time of around 10 minutes. It is observed that controlling the de-binding and sintering conditions is crucial for achieving high-quality metal parts through metal FDM. It is also suggested to split the de-binding and sintering cycles and apply different parameters for each cycle, which may enhance the defect mitigation and quality improvement in metal FDM process. The porosity of specimens sintered in argon and vacuum atmospheres is compared and it is found that vacuum sintering results in lower porosity and higher density than argon sintering. The current study tends to contribute to the understanding of the defect mechanisms and mitigation strategies in metal FDM and has suggested directions for future research and development in this field.

Acknowledgments

The authors acknowledge Mechanical Engineering Department Universiti Teknologi PETRONAS, for providing the necessary support.

Conflict of interest

There is no conflict of interest in this study.

References

[1] Barbosa WS, Wanderley RF, Gioia MM, Gouvea FC, Gonalves FM. Additive or subtractive manufacturing: Analysis and comparison of automotive spare-parts. *Journal of Remanufacturing*. 2022; 12: 153-166. https://doi.org/10.1007/s13243-021-00106-1

[2] Paritala PK, Manchikatla S, Yarlagadda PK. Digital manufacturing-applications past, current, and future trends. *Procedia Engineering*. 2017; 174: 982-991. https://doi.org/10.1016/j.proeng.2017.01.250

[3] ISO, ASTM International. ISO/ASTM 52900. *Additive manufacturing–General principles–Terminology*. International Organization for Standardization; 2015.

[4] Shahrubudin N, Koshy P, Alipal J, Kadir MH, Lee TC. Challenges of 3D printing technology for manufacturing biomedical products: A case study of Malaysian manufacturing firms. *Heliyon*. 2020; 6(4): e03732. https://doi.org/10.1016/j.heliyon.2020.e03734

[5] Butt J. Exploring the interrelationship between additive manufacturing and Industry 4.0. *Designs*. 2020; 4(2): 13. https://doi.org/10.3390/designs4020013

[6] Ngo TD, Kashani A, Imbalzano G, Nguyen KT, Hui D. Additive manufacturing (3D printing): A review of materials, methods, applications and challenges. *Composites Part B: Engineering*. 2018; 143: 172-196. https://doi.org/10.1016/j.compositesb.2018.02.012

[7] Tuncer N, Bose A. Solid-state metal additive manufacturing: A review. *JOM*. 2020; 72(9): 3090-3111. https://doi.org/10.1007/s11837-020-04260-y

[8] Frazier WE. Metal additive manufacturing: A review. *Journal of Materials Engineering and Performance*. 2014; 23: 1917-1928. https://doi.org/10.1007/s11665-014-0958-z

[9] Gonzalez-Gutierrez J, Cano S, Schuschnigg S, Kukla C, Sapkota J, Holzer C. Additive manufacturing of metallic and ceramic components by the material extrusion of highly-filled polymers: A review and future perspectives. *Materials*. 2018; 11(5): 840. https://doi.org/10.3390/ma11050840

[10] Nurhudan AI, Supriadi S, Whulanza Y, Saragih AS. Additive manufacturing of metallic based on extrusion process: A review. *Journal of Manufacturing Processes*. 2021; 66: 228-237. https://doi.org/10.1016/j.jmapro.2021.04.018

[11] Wu G, Langrana NA, Sadanji R, Danforth S. Solid freeform fabrication of metal components using fused deposition of metals. *Materials & Design*. 2002; 23(1): 97-105. https://doi.org/10.1016/S0261-3069(01)00079-6

[12] Kurose T, Abe Y, Santos MV, Kanaya Y, Ishigami A, Tanaka S, et al. Influence of the layer directions on the properties of 316l stainless steel parts fabricated through fused deposition of metals. *Materials*. 2020; 13(11): 2493. https://doi.org/10.3390/ma13112493

[13] Zhang Y, Roch A. Fused filament fabrication and sintering of 17-4PH stainless steel. *Manufacturing Letters*. 2022; 33: 29-32. https://doi.org/10.1016/j.mfglet.2022.06.004

[14] Safka JI, Ackermann M, Machacek J, Seidl MA, Vele FI, Truxova VE. Fabrication process and basic material properties of the BASF Ultrafuse 316LX material. *MM Science Journal*. 2020; 5: 4216-4222. http://doi.org/10.17973/MMSJ.2020_12_2020071

[15] Obadimu SO, Kourousis KI. Microscopic and mesoscopic/macroscopic structural characteristics of material extrusion Steel 316L: influence of the fabrication process. *International Journal of Structural Integrity*. 2022; 14(2): 314-321. https://doi.org/10.1108/IJSI-07-2022-0100

[16] Spiller S, Kolstad SO, Razavi N. Fatigue behavior of 316L stainless steel fabricated via material extrusion additive manufacturing. *Engineering Fracture Mechanics*. 2023; 291: 109544. https://doi.org/10.1016/j.engfracmech.2023.109544

[17] Spiller S, Kolstad SO, Razavi N. Fabrication and characterization of 316L stainless steel components printed with material extrusion additive manufacturing. *Procedia Structural Integrity*. 2022; 42: 1239-1248. https://doi.org/10.1016/j.prostr.2022.12.158

[18] MatterHackers. BASF Ultrafuse 316L Metal 3D Printing Filament. https://www.matterhackers.com/store/l/basf-

ultrafuse-316l-metal-composite-3d-printing-filament-175mm/sk/M9CR1EZH [Accessed 24th July 2023].
[19] Aslam M, Ahmad F, Yusoff PS, Chai WL, Ngeow WC, Nawi MK. Investigation of boron addition on densification and cytotoxicity of powder injection molded 316L stainless steel dental materials. *Arabian Journal for Science and Engineering*. 2016; 41: 4669-4681. https://doi.org/10.1007/s13369-016-2224-1
[20] Gonzalez-Gutierrez J, Godec D, Kukla C, Schlauf T, Burkhardt C, Holzer C. Shaping, debinding and sintering of steel components via fused filament fabrication. In: 16th *International Scientific Conference on Production Engineering—CIM2017*. Zagreb, Croatia: Croatian Association of Production Engineering; 2017. https://www.researchgate.net/publication/317549016
[21] Thompson Y, Gonzalez-Gutierrez J, Kukla C, Felfer P. Fused filament fabrication, debinding and sintering as a low cost additive manufacturing method of 316L stainless steel. *Additive Manufacturing*. 2019; 30: 100861. https://doi.org/10.1016/j.addma.2019.100861